5.3

Efficient Parameter Extraction Techniques for a new Surface-Potential-Based MOS Model for RF Applications

Wenzhi Liang, Ronald van Langevelde, K.G. McCarthy, A. Mathewson

Abstract— **Efficient parameter extraction techniques for a new surface-potential-based MOS model are outlined. The new model is suitable for RF CMOS design because it has improved modelling of surface potential, mobility and conductance. The extraction techniques are based on analytical manipulation of the model equations and allow parameters to be extracted using as few as 12 measurements per device.**

Introduction

This paper deals with the development of efficient parameter extraction techniques for a new surface-potential-based MOS model, which has been shown to be appropriate for RF CMOS[1]. This is the first time quick extraction techniques have been developed for a surface-potential-based model, while they are well established for V_T-based models[2].

The techniques are based on analytical manipulation of the model equations and allow parameters to be extracted directly from a small number of data points. Techniques such as these are vital for statistical characterisation for design for manufacturability (DFM).

Model Background

In the past the main emphasis for MOS model development was an accurate description of the I-V and C-V behaviour and good prediction of quantities such as $\frac{g_m}{I_{DS}}$ and g_{ds} where g_m, I_{DS} and g_{ds} are the transconductance, drain current and output conductance respectively. With the use of MOS devices for RF applications, it is necessary to have models which can predict 2nd and 3rd order distortion, which depend on the 2nd and 3rd derivatives of current with respect to V_{DS} and V_{GS}. The new model, which has been named MOS Model 11[3], meets these requirements by using (a) an improved surface potential model[4], (b) physically based mobility models[5] and (c) a more accurate description of conductance[6].

The ability of the model to simulate 1st (HD1), 2nd (HD2) and 3rd (HD3) order harmonics is seen in Fig. 1 and 2, which show the harmonic content of the drain current as a function of V_{GS} with a 1kHz sinusoidal input applied in series with the DC gate bias.

W. Liang and A. Mathewson are with the NMRC, Cork, Ireland. E-mail: liang.wenzhi@nmrc.ie, alan.mathewson@nmrc.ie

R. van Langevelde is with Philips Research Laboratories, Eindhoven, the Netherlands. E-mail: ronald.van.langevelde@philips.com

K.G. McCarthy is with the Dept. of Electrical and Electronics Engineering, University College Cork, Ireland. E-mail: kevin.mccarthy@ucc.ie

These abilities have also been tested at RF-frequencies and shown good results[7].

The model also includes small-geometry effects such as drain induced barrier lowering (DIBL), self-heating and static feedback . These abilities make this model very suitable for mixed signal design and low-power low-voltage applications.

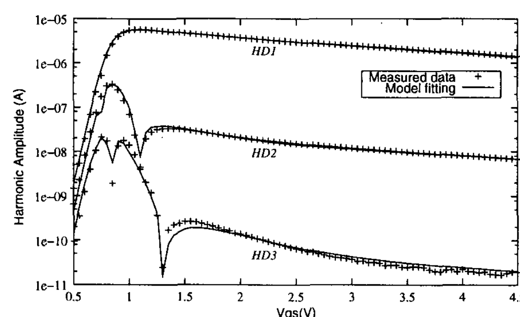

Fig. 1. Harmonic distortion in drain current I_{DS} with a sinusoidal voltage applied to the gate terminal at low drain bias. NMOS, 10μm/1μm, V_{SB}=0V, V_{DS}=0.1V.

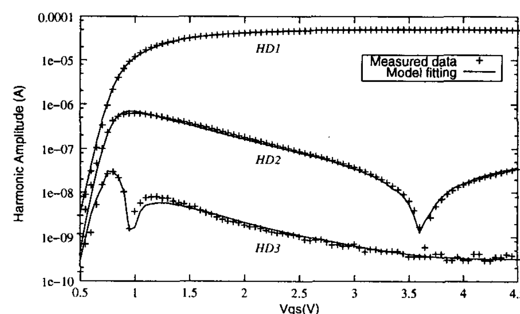

Fig. 2. Harmonic distortion in drain current I_{DS} with a sinusoidal voltage applied to the gate terminal at low drain bias. NMOS, 10μm/1μm, V_{SB}=0V, V_{DS}=3V.

Parameter Extraction Methodology

Table I shows the list of parameters extracted while the strategy is shown in Fig. 3. A long channel device is used to extract the mobility coefficients associated with phonon and surface roughness scattering. A slightly different strategy is used for short devices - these are used for the extraction of the self-heating and series resistance parameters.

0-7803-6511-9/01/$10.00©2001 IEEE 01CH37153

Parameter	Description
V_{FB}	Flat-band voltage
k_o	Body effect coefficient
β	Gain factor
θ_{ph}	Coefficient of the mobility reduction due to phonon scattering
θ_{sr}	Coefficient of the mobility reduction due to surface roughness scattering
σ_{dibl}	Drain induced barrier lowering parameter
θ_n / θ_p	Velocity saturation parameter due to optical/acoustic phonon scattering
η_{mob}	Depletion charge mobility effect
θ_R	Series resistance parameter
σ_{sf}	Static feedback parameter
θ_{TH}	Coefficient of self-heating
α	Channel length modulation factor
a_1, a_2, a_3	Avalanche parameters

TABLE I
LIST OF MODEL PARAMETERS FOR A MOSFET WITH A GIVEN GEOMETRY.

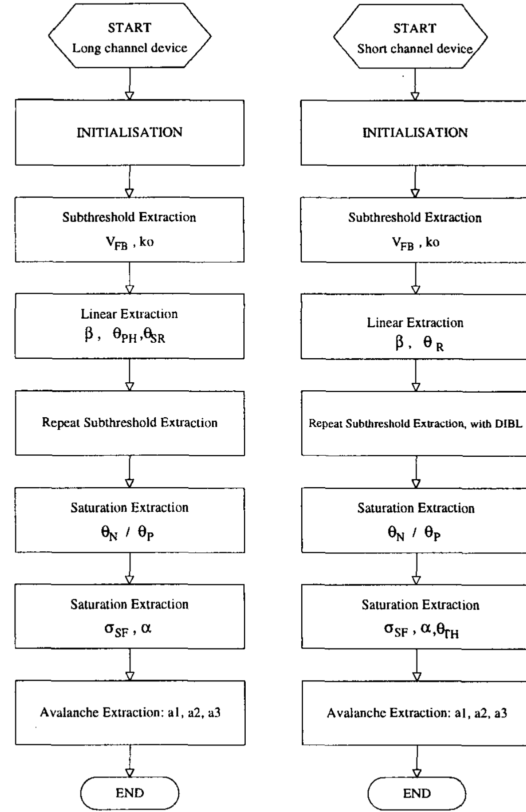

Fig. 3. Parameter extraction procedure for long and short channel lengths.

The method used is to closely examine the model equations in each of the operating regions (i.e. subthreshold, linear and saturation) to determine if a simplified equation set can be used. This is then analytically manipulated to determine a direct relationship between the current measured at selected bias points and the model parameters. The resulting algorithms are described in more detail in the following sections.

The general model equation for drain current is:

$$I_{DS} = \frac{\beta \cdot (I_{drift} + I_{diff})}{G_{vsat} \cdot G_{\Delta L} + G_{R+Th}} \qquad (1)$$

where the terms represent the gain factor (β), the drift current (I_{drift}), the diffusion current (I_{diff}), mobility degradation and velocity saturation (G_{vsat}), channel length modulation ($G_{\Delta L}$) and series resistance and self-heating (G_{R+Th}).

The two most fundamental model parameters are the flat band voltage (V_{FB}) and body effect factor (k_o), which determine the threshold voltage V_T. In V_T-based models[1], the threshold voltage parameters are normally determined from linear region I_{DS}-V_{GS} characteristics at various body-bias values. In this surface-potential-based model, however, V_{FB} and k_o are determined from two measurements in the subthreshold region as illustrated in Fig. 4. Note that most of the data points in Fig. 4 (and in all the other I-V curves) have been measured to illustrate the quality of the fit and are not used for parameter extraction. The algorithm is illustrated in Fig. 5. The subthreshold current depends on V_{FB}, k_o and β. An initial approximation for β is required during the extraction of V_{FB} and k_o. The

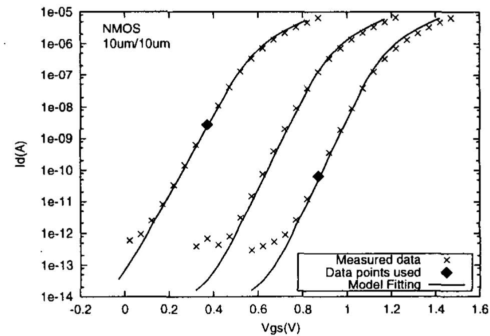

Fig. 4. Extraction in subthreshold for long device (V_{SB}=0, 1.65, 3.3V): data points used for quick extraction of parameters V_{FB} and k_o and resulting fit.

performance and robustness of the technique are illustrated in Fig. 6 and Fig. 7 respectively. Fig. 6 shows that the number of iterations needed is below 10 regardless of the intial value of k_o while Fig. 7 shows that the final values of the V_{FB} and k_o are independent of the initial guess for k_o.

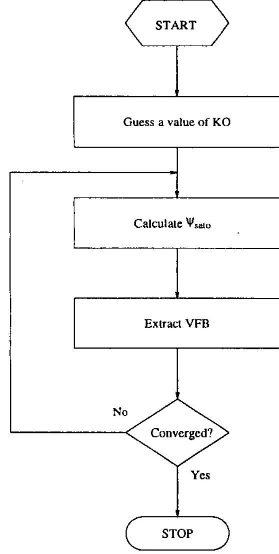

Fig. 5. Details of the subthreshold parameter extraction algorithm.

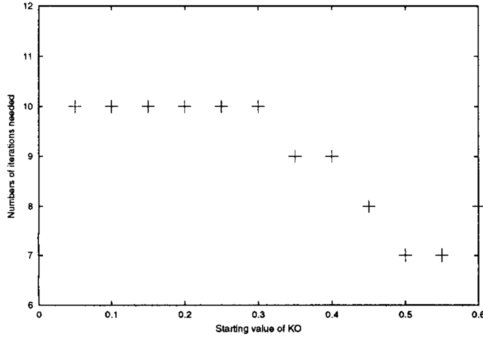

Fig. 6. Number of iterations needed to come to a convergence.

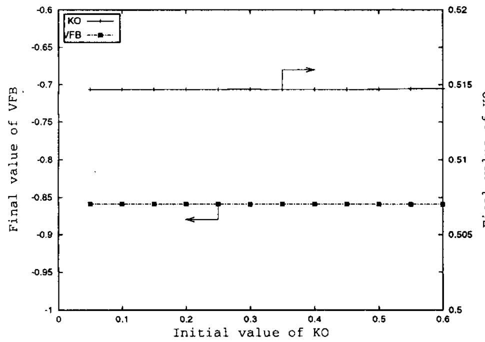

Fig. 7. Extraction algorithm for V_{FB} and k_o: variation of extracted parameters with initial value of k_o.

Since drain current I_{DS} is proportional to gain factor β, parameters V_{FB} and k_o are re-extracted after the extraction of gain factor β as shown in the flowchart (Fig. 3).

Fig. 8 illustrates the data points used for the subthreshold extraction of a short device and the resulting fit. For this device, an extra data point is measured for a large V_{DS} to extract the drain induced barrier lowering (DIBL) parameter, σ_{dibl}.

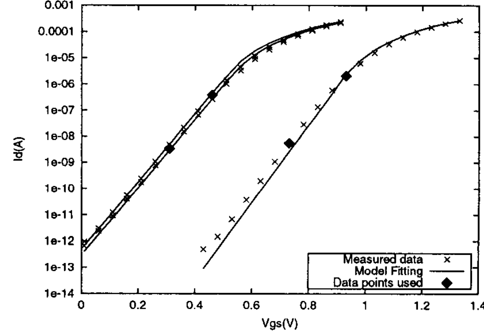

Fig. 8. Extraction of subthreshold parameters for short device (2 data points at V_{DS}=0.1V, V_{SB}=0V, 1 at V_{DS}=0.1V, V_{SB}=3.3V and 1 at V_{DS}=2.15V, V_{SB}=0V.

In the linear region for a long device, eq. (1) can be simplified by ignoring diffusion current, channel length modulation and velocity saturation, thus creating a new equation which can be analytically manipulated to determine the gain and mobility reduction parameters from 3 measurement points. The simplified version of the current equation given in eq. (2) is thus obtained by setting the channel length modulation term to 1 ($G_{\Delta L} = 1$), ignoring the influence of the I_{diff} and G_{R+Th} and by replacing G_{vsat} by G_{mob} so that velocity saturation effects are neglected.

$$I_{DS} = \frac{\beta \cdot I_{drift}}{G_{mob}} \tag{2}$$

Here, G_{mob} is the gate voltage induced mobility degradation factor[5]:

$$G_{mob} = 1 + \sqrt{(\theta_{ph} \cdot E_{eff})^{2/3} + (\theta_{sr} \cdot E_{eff})^4} \tag{3}$$

The parameters representing gain (β), phonon scattering (θ_{ph}) and surface roughness scattering (θ_{sr}) are obtained from 3 measurements at zero back bias in the linear region as shown in Fig. 9. β is taken out of consideration first by taking the ratio of these 3 data points so that eq. (4) and 5 are derived.

$$G_{mob_1} = G_{mob_0} \cdot \frac{I_{DS_0} \cdot (I_{drift_1} + I_{diff_1})}{I_{DS_1} \cdot (I_{drift_0} + I_{diff_0})} \tag{4}$$

$$G_{mob_2} = G_{mob_0} \cdot \frac{I_{DS_0} \cdot (I_{drift_2} + I_{diff_2})}{I_{DS_2} \cdot (I_{drift_0} + I_{diff_0})} \tag{5}$$

where the factor G_{mob} represents the effect of mobility degradation, which depends on the bias condition as well as the value of θ_{sr} and θ_{ph}. In eq. (4) and (5) the subscripts 0, 1, 2 refer to the bias points used.
Inserting the definition of G_{mob} into eq. (4) and eq. (5) and doing some manipulation, a linear relationship can be reached:

$$\theta_{ph}{}^{2/3} = A \cdot \theta_{sr}{}^4 + B \tag{6}$$

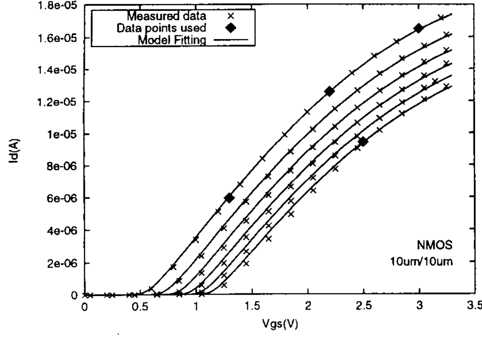

Fig. 9. Extraction in linear region for long device (V_{SB}=0, 0.66, 1.32, 1.98, 2.64, 3.3V): data points used for quick extraction of parameters β, θ_{ph}, θ_{sr}, and η_{mob} and resulting fit.

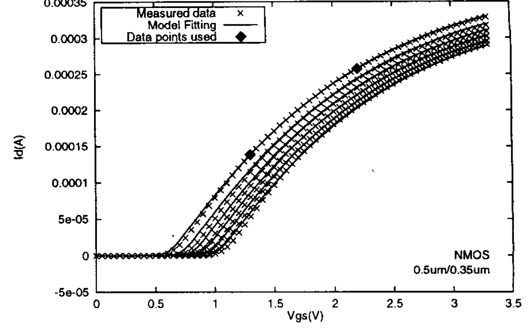

Fig. 10. Extraction in the linear region for short device (V_{SB}=0, 0.66, 1.32, 1.98, 2.65, 3.3V): data points used for quick extraction of β, θ_{sr} and result fit.

where A and B are constants with a given bias condition.

Inserting this linear equation into eq. (4) or eq. (5), a value of θ_{sr} can be extracted and then θ_{ph} can be solved. Finally β can be extracted using these values.

The parameter η_{mob} which represents the influence of the depletion charge on the mobility is then extracted from a single measurement at non-zero V_{SB} in the linear region as shown also.

G_{mob} can be determined from one data point:

$$G_{mob} = \beta \cdot \frac{(I_{drift} + I_{diff})}{I_{DS}} - G_{R+TH} \tag{7}$$

In turn, E_{eff} can be calculated with the value of G_{mob} (for an N-type device) using eq. (3):

$$E_{eff} = \left(\frac{(G_{mob} - 1)^2 - (\theta_{ph} \cdot E_{eff})^{2/3}}{\theta_{sr}{}^4} \right)^{1/4} \tag{8}$$

Finally, η_{mob} can be extracted by eq. (9):

$$\eta_{mob} = \frac{E_{eff} - V_{GS1}}{k_o \cdot \sqrt{V_{SB} + \frac{1}{2} \cdot V_{DS} + \phi_B}} \tag{9}$$

The extraction of η_{mob} requires one measurement at non-zero back bias as illustrated in Fig. 9 which illustrates the fit quality to the linear region.

For the short device, the values of θ_{ph}, θ_{sr} and η_{mob} which were extracted from the long device can be used because they have the same physical origin. However, series resistance comes into play so, θ_R must be extracted from the linear region. Fig. 10 shows that 2 measured data points are used to determine β and θ_R at the same time for a short device from the linear region characteristic. In eq. (1), G_{R+Th} can now be defined as:

$$G_{R+Th} = \theta_R \cdot V_{GS1} \tag{10}$$

The ratio of 2 current values can again be taken to eliminate β and the resulting equation is then manipulated to generate the value of θ_R by eq. (11).

$$\theta_R = \frac{ii \cdot G_{mob_0} - G_{mob_1}}{V_{GS1_1} - V_{GS1_0}} \tag{11}$$

where:

$$ii = \frac{I_{DS_0} \cdot (I_{drift_1} + I_{diff_1})}{I_{DS_1} \cdot (I_{drift_0} + I_{diff_0})} \tag{12}$$

and then β can be derived by eq. (13):

$$\beta = \frac{I_{DS_0} \cdot (G_{mob_0} + \theta_R \cdot V_{GS1_0})}{I_{drift_0} + I_{diff_0}} \tag{13}$$

In the saturation region, the current can be modelled by eq. (14):

$$I_{DS} = \frac{\beta \cdot I_{drift}}{G_{vsat} \cdot G_{\Delta L} + G_{R+Th}} \tag{14}$$

The term $G_{\Delta L}$ represents channel length modulation, which is determined by the parameter α. G_{R+Th} represents series resistance, self-heating, which are determined by θ_R and θ_{TH} respectively.

Equation 14 can be manipulated in a similar fashion to that which was performed for the linear and subthreshold regions to determine analytical expressions for the saturation parameters. Fig. 11 illustrates the extraction of the saturation region parameter, θ_n from one I_{DS}-V_{DS} measurement from the saturation region of a long channel device and the resulting fit. Fig. 12 illustrates the extraction of the saturation region parameters α and σ_{sf} from two g_{ds} measurements from the saturation region of a long channel device and the resulting fit.

Fig. 13 illustrates the extraction of the saturation parameters α, σ_{sf} and θ_{TH} from three data points from the saturation region of a short channel device and the resulting fit.

Measurements at high V_{DS} are used to determine the avalanche current parameters (a_1, a_2 and a_3) with the resulting fit shown in Fig. 14. The avalanche current can be calculated by eq. (15).

$$I_{avl} = a_1 \cdot I_{DS} \cdot \exp\left(-\frac{a_2}{V_{DS} - a_3 \cdot V_{DSAT}} \right) \tag{15}$$

where I_{DS} is the channel current and V_{DSAT} is the saturation voltage whose definition can be found elsewhere [1]. By measuring three values of avalanche current, I_{avl} and suitable manipulation of eq. (15), a simplified equation

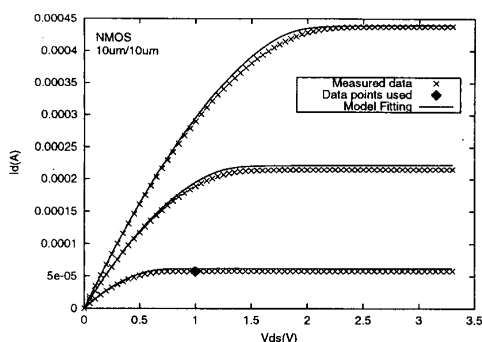

Fig. 11. Extraction in saturation region for long device (V_{GS}=1.5, 2.4, 3.3V): data points used for quick extraction of parameter θ_n and resulting fit.

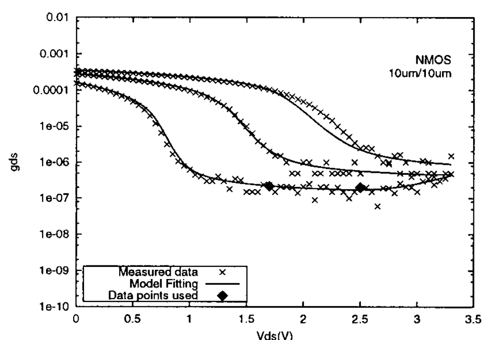

Fig. 12. Output conductance parameters extraction for long device (V_{GS}=1.5, 2.4, 3.3V): data points used for quick extraction of α, σ_{sf} and resulting fit.

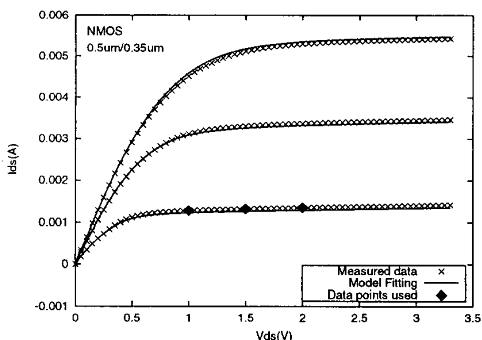

Fig. 13. Extraction of output conductance parameters for short device (V_{GS}=1.5, 2.4, 3.3V): data points used for quick extraction of α, σ_{sf}, θ_{TH} and resulting fit.

set can be determined and solved to give the avalanche parameters.

To insure good quality fit, some steps are repeated as seen in the flowcharts (Fig. 3).

Summary

This paper discussed quick extraction procedures for a new surface-potential-based MOS model. The analytical expressions and data requirements were discussed for each

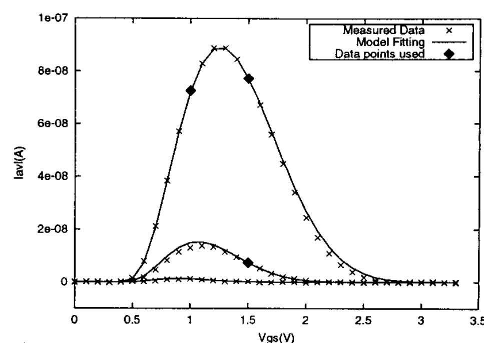

Fig. 14. Avalanche parameter extraction (V_{DS}=2.3, 2.8, 3.3V): data points used for quick extraction of parameters a_1, a_2 and a_3 and resulting fit.

region and the resulting fits illustrated for both long and short channel devices.

References

[1] *A Compact MOSFET Model for Distortion Analysis in Analog Circuit Design.* R. van Langevelde. Ph.D. Thesis. Technische Universiteit Eindhoven, 1998.

[2] *Statistical Characterisation of 0.18μm Low-power CMOS Process using Efficient Parameter Extraction.* K.G. McCarthy, E.V. Saavedra Diaz, D.B.M Klaassen, A. Mathewson. Proc. ICMTS 1998, pp 127-131.

[3] *RF-Distortion in Deep-Submicron CMOS Technologies.* R. van Langevelde et al. IEDM Dig. 2000, pp. 807-810, 2000.

[4] *An explicit surface-potential-based MOSFET model for circuit simulation.* R. van Langevelde, F.M. Klaassen. Solid-State Electronics, Vol. 44 (2000) pp. 409-418.

[5] *Effect of Gate-Field Dependent Mobility Degradation on Distortion Analysis in MOSFET's.* R. van Langevelde, F.M. Klaassen. IEEE Trans. Electron Devices, Vol. ED-44, No.11, pp. 2044-2052, 1997.

[6] *Accurate Drain Conductance Modelling for Distortion Analysis in MOSFETs.* R. van Langevelde, F.M. Klaassen. IEDM 1997 Tech. Dig., pp. 313-316, 1997.

[7] *RF Distortion Characterisation of Sub-Micron CMOS.* L.F. Tiemeijer et al. ESSDERC2000, pp. 464-467, 2000.